

# Reductive amination of 2-propanol to monoisopropylamine over Co/ $\gamma$ -Al<sub>2</sub>O<sub>3</sub> catalysts

Jun Hee Cho<sup>a</sup>, Jung Hyun Park<sup>a</sup>, Tae-Sun Chang<sup>b</sup>, Gon Seo<sup>c</sup>, Chae-Ho Shin<sup>a,\*</sup>

<sup>a</sup> Department of Chemical Engineering, Chungbuk National University, Chungbuk 361-763, Republic of Korea

<sup>b</sup> Environment & Resources Research Center, Korea Research Institute of Chemical Technology, Daejeon 305-353, Republic of Korea

<sup>c</sup> School of Applied Chemical Engineering and the Institute for Catalysis Research, Chonnam National University, Gwangju 500-757, Republic of Korea

## ARTICLE INFO

### Article history:

Received 10 November 2011

Received in revised form 6 January 2012

Accepted 7 January 2012

Available online 16 January 2012

### Keywords:

2-Propanol

Acetone

Reductive amination

Cobalt

Monoisopropylamine

## ABSTRACT

Co/ $\gamma$ -Al<sub>2</sub>O<sub>3</sub> catalysts with 4–27 wt% cobalt loadings were prepared by incipient-wetness impregnation and used to catalyze the synthesis of monoisopropylamine by the reductive amination of 2-propanol in the presence of hydrogen and ammonia. The catalysts were characterized by X-ray diffraction, H<sub>2</sub>-temperature programmed reduction, N<sub>2</sub>-sorption, and H<sub>2</sub>-chemisorption. 23 wt% Co loading resulted in the highest catalytic activity and a long-term stability of up to 100 h on stream. 2-Propanol conversion was related to the exposed metal surface area and the number of exposed cobalt atoms. In the absence of hydrogen, the catalyst was progressively deactivated; its initial activity and selectivity were completely recovered upon re-exposure to hydrogen. The deactivation was due to the formation of metal nitride caused by the strong adsorption of ammonia on the surface of the metal phase. Excess hydrogen hindered the phase transition to metal nitride, preventing deactivation.

© 2012 Elsevier B.V. All rights reserved.

## 1. Introduction

The reductive amination of aliphatic alcohols is used to produce alkylamines that can be used as intermediates for the synthesis of herbicides, insecticides, pharmaceutical chemicals, corrosion inhibitors, plastics, and rubber chemicals [1–5]. The process can proceed by hydrogenation–dehydrogenation over nickel, cobalt, copper, and solid acid catalysts; it is metal-catalyzed, with alcohol conversion being proportional to the exposed metal surface area [6–10].

Monoisopropylamine (MIPA) is generally synthesized by contacting 2-propanol and ammonia at high pressure ( $\approx$ 20 bar) [11,12]. The reductive amination of 2-propanol over supported metal catalysts is complex and involves dehydrogenation, condensation, and hydrogenation steps (Scheme 1), with the dehydrogenation of 2-propanol to acetone being the rate determining step. The first and last redox processes are catalyzed by the metal; the reaction of the intermediate carbonyl compound with NH<sub>3</sub> to form an imine can be accelerated by acid/base catalysis [13–16].

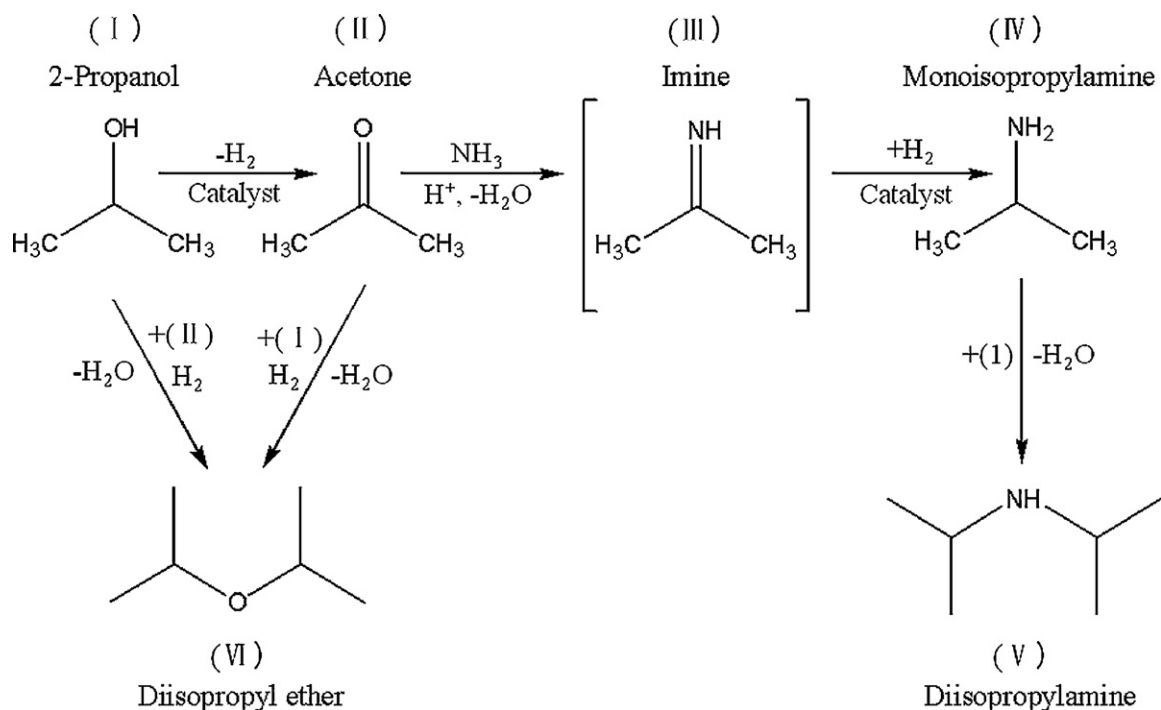
Cobalt-based catalysts are industrially important in a variety of reactions. The redox properties of cobalt species allow their use in either the reduced state for Fischer–Tropsch synthesis and

hydrogenation and dehydrogenation reactions or the oxidized state for oxidation [17–21]. Gardner et al. [22] reported cobalt catalysts with higher activity than supported nickel catalysts for reductive amination with high metal loadings and high space velocity at relatively low temperature. However, conversion and yield are usually low in the synthesis of alkylamines from alcohols and ammonia at atmospheric pressure.

In batch-type reductive amination, industrial separation and recycling of catalyst and by-product are difficult. The reductive amination of alcohols has been widely investigated. Dobson et al. [23] reported the reductive amination of 2-propanol over supported nickel–palladium–ruthenium catalysts at high pressures ( $\approx$ 50 bar) in an autoclave. However, most studies were focused on methanol, ethanol and cyclohexanol [5,24–26]. There are few reports regarding the influence of reaction parameters on the reductive amination of 2-propanol over supported metal catalysts.

This work reports the catalytic properties of Co/ $\gamma$ -Al<sub>2</sub>O<sub>3</sub> catalysts for the reductive amination of 2-propanol in the presence of ammonia and hydrogen at atmospheric pressure. 2-Propanol conversion and selectivities to MIPA, acetone, diisopropylamine (DIPA), and diisopropylether (DIPE) were evaluated on Co/ $\gamma$ -Al<sub>2</sub>O<sub>3</sub> catalysts with various Co loadings. Various hydrogen and ammonia feed compositions and reaction temperatures were tested. Calcined and reduced catalysts were characterized by X-ray diffraction (XRD), H<sub>2</sub>-temperature programmed reduction (H<sub>2</sub>-TPR), NH<sub>3</sub>-temperature programmed desorption (NH<sub>3</sub>-TPD), N<sub>2</sub>-sorption, and H<sub>2</sub>-chemisorption.

\* Corresponding author. Tel.: +82 43 261 2376; fax: +82 43 269 2370.  
E-mail address: [chshin@chungbuk.ac.kr](mailto:chshin@chungbuk.ac.kr) (C.-H. Shin).



**Scheme 1.** Reaction pathways in the reductive amination of 2-propanol.

## 2. Experimental

### 2.1. Catalyst preparation

Co/ $\gamma$ -Al<sub>2</sub>O<sub>3</sub> catalysts with 4–27 wt% cobalt loadings were prepared by incipient wetness impregnation using Co(NO<sub>3</sub>)<sub>3</sub>·6H<sub>2</sub>O (Sigma–Aldrich) solution on commercial  $\gamma$ -Al<sub>2</sub>O<sub>3</sub> (Procatalyse, 194 m<sup>2</sup> g<sup>-1</sup>). The impregnated catalysts were dried at 100 °C overnight and subsequently calcined at 500 °C for 2 h in a muffle furnace under flowing air (200 cm<sup>3</sup> min<sup>-1</sup>). The final catalysts are labeled Co(x)/Al<sub>2</sub>O<sub>3</sub>, with x denoting the weight percent of Co metal (4, 11, 17, 23 or 27 wt%).

### 2.2. Catalyst characterization

The catalysts were degassed for 6 h at 250 °C before their BET surface areas, pore volumes and pore size distributions were determined by N<sub>2</sub> physisorption at –196 °C using Micromeritics ASAP2020 apparatus. Surface areas were calculated over a 0.01–0.2 relative pressure range. Pore size distributions were calculated from the desorption branch using BJH formulism. X-ray diffraction (XRD) patterns were recorded on a Rigaku D/MAX 2500H diffractometer using Cu K $\alpha$  radiation to identify the phases of Co/ $\gamma$ -Al<sub>2</sub>O<sub>3</sub>. Co particle sizes were determined from the broadening of the diffraction peaks using Scherrer's equation. H<sub>2</sub>-temperature-programmed reduction (H<sub>2</sub>-TPR) using a Micromeritics AutoChem II 2920 instrument determined the reducibility of cobalt oxides. Before measurement, each 0.1 g sample was pretreated under flowing He (50 cm<sup>3</sup> min<sup>-1</sup>) up to 400 °C and held for 1 h to remove adsorbed water and other contaminants before being cooled to 30 °C under flowing He. Reducing gas containing 5% H<sub>2</sub>/Ar mixture (50 cm<sup>3</sup> min<sup>-1</sup>) was then passed with 15 °C min<sup>-1</sup> heating to 800 °C. A thermal conductivity detector determined the amount of H<sub>2</sub> consumed.

The dispersion of cobalt and metal surface area was measured by H<sub>2</sub> chemisorption at 100 °C under static conditions using a Micromeritics ASAP 2020C instrument equipped with a high

vacuum pump providing 10<sup>-6</sup> Torr. Prior to adsorption experiments, each 0.3 g sample was reduced at 600 °C for 3 h. H<sub>2</sub> chemisorption uptakes were separately determined as the difference of two successive isotherm measurements. Metal dispersion and cobalt metal surface area were calculated assuming a H/Co stoichiometry of 1. The degree of reduction was determined by O<sub>2</sub> titration and the sizes of the cobalt particles were corrected considering the degree of reduction, which was determined by the following equation: [the amount of O<sub>2</sub> consumption (mmol O<sub>2</sub>; 3Co + 2O<sub>2</sub> → Co<sub>3</sub>O<sub>4</sub>)]/[the theoretical amount of H<sub>2</sub> consumption with the assumption of fully reduced cobalt oxides (mmol H<sub>2</sub>; Co<sub>3</sub>O<sub>4</sub> + 4H<sub>2</sub> → 3Co + 4H<sub>2</sub>O)] × 100 [17,27].

To identify the species adsorbed over the catalysts, the evolution of NH<sub>3</sub> and H<sub>2</sub> were examined during TPD/TPR using a Balzers QMS200 quadruple mass spectrometer (QMS). The QMS signals of •NH<sub>3</sub> (*m/e* = 17) and •H<sub>2</sub> (*m/e* = 2) were recorded. Prior to measurement, samples were reduced under a 50 cm<sup>3</sup> min<sup>-1</sup> H<sub>2</sub> flow at 600 °C for 3 h with heating at 10 °C min<sup>-1</sup>.

### 2.3. Catalytic activity tests

All catalytic experiments were performed at atmospheric pressure under a continuous flow in a fixed bed microreactor. Prior to testing, the catalysts were activated at 600 °C for 3 h under a 50 cm<sup>3</sup> min<sup>-1</sup> flow of purified H<sub>2</sub> and kept at the desired temperature to establish a standard operating procedure, allowing time for the product distribution to stabilize. Standard reaction procedures were considered under the following conditions: catalyst = 0.1 g; *T* = 210 °C; WHSV = 4.29 h<sup>-1</sup>, feed composition of 2-propanol/NH<sub>3</sub>/H<sub>2</sub>/N<sub>2</sub> = 1/4/6/22.8. Molar ratios of H<sub>2</sub>/2-propanol and NH<sub>3</sub>/2-propanol were varied in the ranges 2–12, and 2–16, respectively, and reaction temperatures of 170–250 °C were tested. The total flow rate was fixed at 90 cm<sup>3</sup> min<sup>-1</sup> using nitrogen diluents to maintain constant partial pressures of the other reactants. The partial pressure of 2-propanol was constant 3 kPa. The reaction products were analyzed on-line using a Chrompack-CP-9001

**Table 1**  
Physical properties of Co/ $\gamma$ -Al<sub>2</sub>O<sub>3</sub> catalysts.

Co loading (wt%)	Surface area (m <sup>2</sup> g <sup>-1</sup> )	Pore volume (cm <sup>3</sup> g <sup>-1</sup> )	Pore size (nm)
4	163	0.60	15
11	144	0.50	14
17	137	0.40	12
23	124	0.38	12
27	119	0.34	11

gas chromatograph equipped with a CP-Volamine capillary column (60 m × 0.32 mm) and a flame ionization detector.

The conversion of 2-propanol and selectivity to MIPA was defined as follows:

Conversion (%)

$$= \frac{2\text{-propanol}_{\text{feed}} (\text{mol}) - 2\text{-propanol}_{\text{unreacted}} (\text{mol})}{2\text{-propanol}_{\text{feed}} (\text{mol})} \times 100$$

Selectivity (%)

$$= \frac{\text{MIPA}_{\text{produced}} (\text{mol})}{2\text{-propanol}_{\text{feed}} (\text{mol}) - 2\text{-propanol}_{\text{unreacted}} (\text{mol})} \times 100$$

### 3. Results and discussion

#### 3.1. Characterization

The physical properties of Co/ $\gamma$ -Al<sub>2</sub>O<sub>3</sub> catalysts calcined are summarized in Table 1. The BET surface areas of the catalysts decreased with increasing cobalt loading. The specific surface area, pore volume and pore size were progressively decreased as the cobalt loading increased from 4 to 27 wt%. This may be due to partial blockage of the Al<sub>2</sub>O<sub>3</sub> pores by impregnation and successive thermal treatment of corresponding catalysts.

The XRD patterns of the various Co/ $\gamma$ -Al<sub>2</sub>O<sub>3</sub> catalysts calcined at 500 °C and reduced at 600 °C (Fig. 1) showed diffraction peaks at  $2\theta = 37.6^\circ$ ,  $45.8^\circ$  and  $66.8^\circ$  from the  $\gamma$ -Al<sub>2</sub>O<sub>3</sub> (JCPDS 29-0063). The calcined catalysts showed a characteristic reflection peak at  $2\theta = 36.8^\circ$  from Co<sub>3</sub>O<sub>4</sub> phase (JCPDS 42-1467). The XRD patterns show no new crystalline compounds formed between the cobalt oxide and the  $\gamma$ -Al<sub>2</sub>O<sub>3</sub>. The reduced Co/ $\gamma$ -Al<sub>2</sub>O<sub>3</sub> catalysts showed characteristics peaks of metallic Co (JCPDS 15-0806) and  $\gamma$ -Al<sub>2</sub>O<sub>3</sub>. The sizes of the metallic Co particles (Table 2) were determined from the broadening of the diffraction peaks using Scherrer's equation. The calcined Co<sub>3</sub>O<sub>4</sub>/ $\gamma$ -Al<sub>2</sub>O<sub>3</sub> showed Co<sub>3</sub>O<sub>4</sub> particles that increased from 8 to 20 nm with increasing Co loading. High-temperature reduction at 600 °C resulted in smaller metallic Co particles, 8–15 nm. Reduced Co(11)/Al<sub>2</sub>O<sub>3</sub> exhibited the smallest Co particles of 8.1 nm and reduced Co(27)/Al<sub>2</sub>O<sub>3</sub> contained the largest Co particles of 14.8 nm. The Co species were more likely to sinter to yield larger Co particles at increased cobalt loading. This result appears to agree with the data on the degree of metal dispersion (Table 2).

H<sub>2</sub>-TPR profiles of the various catalysts calcined at 500 °C (Fig. 2) show two main broad reduction peaks at 300–500 °C and 600–750 °C. The reduction peaks for the bulk Co<sub>3</sub>O<sub>4</sub> were assigned to the two-step reduction of Co<sub>3</sub>O<sub>4</sub> to CoO to Co<sup>0</sup> [5,28], with the first being attributed to the reduction of bulk Co<sub>3</sub>O<sub>4</sub> (Co<sup>3+</sup> → Co<sup>2+</sup> → Co<sup>0</sup>) and the higher temperature peak corresponding to the reduction of cobalt aluminate (CoO–Al<sub>2</sub>O<sub>3</sub>) formed on the catalyst surface layer [29]. Alumina supported cobalt catalysts have been reported to form cobalt aluminate that can hinder the complete reduction of the cobalt species [30]. Therefore, the second

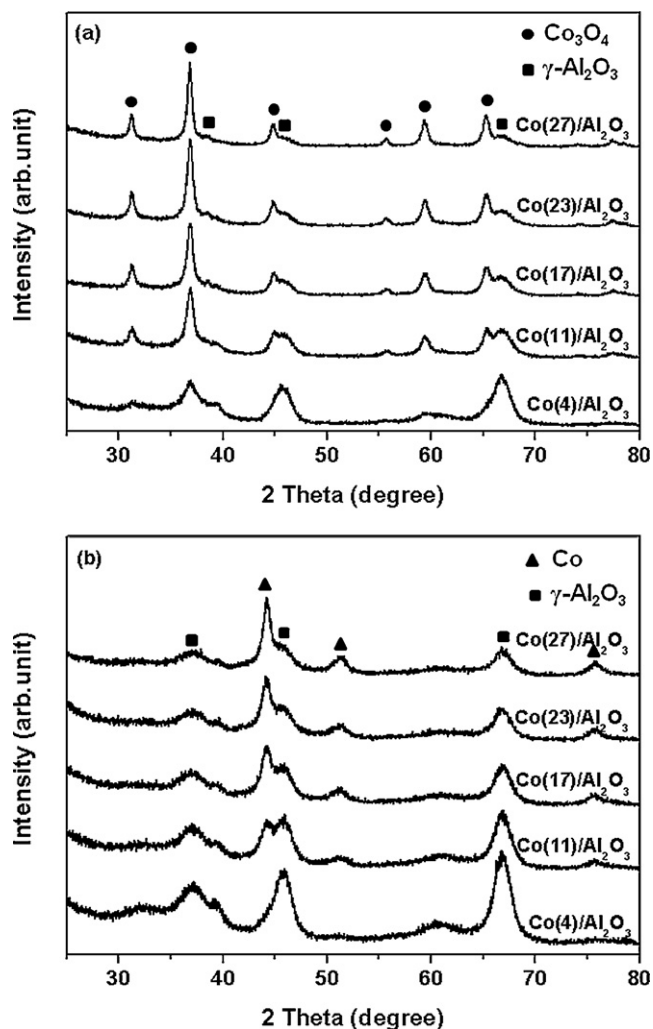


**Fig. 1.** XRD patterns of Co/ $\gamma$ -Al<sub>2</sub>O<sub>3</sub> catalysts with various cobalt contents: (a) calcined at 500 °C for 2 h, and (b) reduced at 600 °C for 3 h.

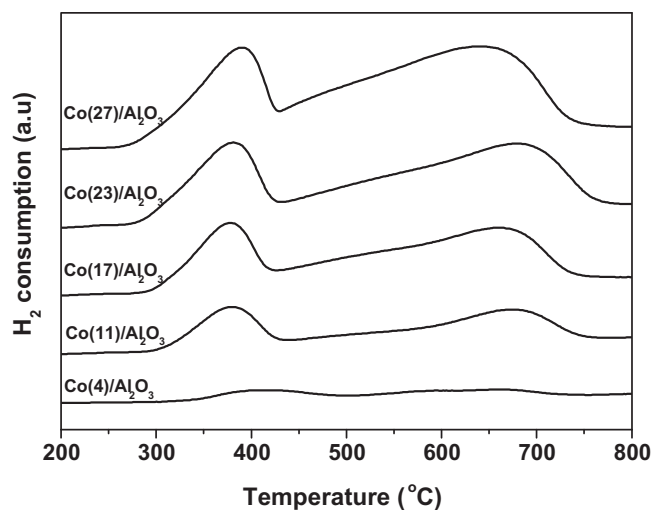


**Fig. 2.** H<sub>2</sub>-TPR profiles of Co/ $\gamma$ -Al<sub>2</sub>O<sub>3</sub> catalysts calcined at 500 °C for 2 h.

**Table 2**  
Cobalt particle size and dispersion measured by H<sub>2</sub> chemisorption and XRD analysis, and reduction degree of cobalt oxides.

Co loading (wt.%)	XRD		O <sub>2</sub> titration		H <sub>2</sub> chemisorption		Metallic surface area (m <sup>2</sup> g <sub>cat</sub> <sup>-1</sup> )	
	Particle size of Co <sub>3</sub> O <sub>4</sub> (nm)	Particle size of Co (nm)	Reduction degree <sup>a</sup> (%)	Uncorrected		Corrected		
				Dispersion (%)	Particle size (nm)	Dispersion <sup>b</sup> (%)		Particle size <sup>c</sup> (nm)
4	8.1	8.2	10.7	0.8	120.1	7.7	0.2	
11	13.6	8.1	20.0	1.6	62.2	8.0	1.2	
17	14.8	11.1	20.6	1.4	70.1	6.9	1.6	
23	15.6	13.9	22.0	1.3	72.0	6.3	2.2	
27	19.5	14.8	23.8	1.1	90.2	4.6	2.0	

<sup>a</sup> Calculated from O<sub>2</sub> uptake.

<sup>b</sup> Corrected dispersion (D, %) = surface Co<sup>0</sup> atom/total reduced Co<sup>0</sup> atom × 100 = surface Co<sup>0</sup> atom/(total Co atom × fraction of reduced Co<sup>0</sup> atom) × 100.

<sup>c</sup> Corrected metallic Co particle size = uncorrected Co diameter × fraction of reduced Co<sup>0</sup> atom.

peak can be assigned to the cobalt oxide layer contacting the alumina surface. Increasing cobalt loading increased the intensity and area of the first reduction peak and shifted it to lower temperatures, indicating that the decrease of interactions between the Co<sub>3</sub>O<sub>4</sub> and the γ-Al<sub>2</sub>O<sub>3</sub> support [31]. The increasing intensity suggests the more facile reduction of larger cobalt oxide particles within the size range of 8.1–19.5 nm (XRD). Therefore, particle size and cobalt loading affected the degree of reduction due to differences in their interactions with alumina.

Measurement of H<sub>2</sub> chemisorption on the reduced catalysts allowed quantification of the number of cobalt metal sites, cobalt dispersion and average metal particle size. The results of H<sub>2</sub> chemisorption measurement were corrected by the degree of reduction measured by O<sub>2</sub> titration (Table 2). The cobalt particles, when corrected by considering the degree of reduction, were smallest (ca. 12.5 nm) in Co(11)/Al<sub>2</sub>O<sub>3</sub>. Particle size increased from 12.5 to 21.5 nm with increasing cobalt loading. The cobalt particle sizes were in good agreement with the results of the XRD analysis, which showed the smallest Co particles of 8.1 nm exhibited by Co(11)/γ-Al<sub>2</sub>O<sub>3</sub> and the largest of 14.8 nm shown by Co(27)/Al<sub>2</sub>O<sub>3</sub>. Comparison of the O<sub>2</sub> titrations of cobalt oxide on alumina supports shows increasing reduction with increasing cobalt loading, in agreement with the H<sub>2</sub>-TPR results that showed shifting to lower temperatures of the first peaks corresponding to the reduction of cobalt oxide. The low degree of reduction of the Co/γ-Al<sub>2</sub>O<sub>3</sub> catalyst was attributed to the small cobalt oxide particles that could easily form cobalt–aluminate during calcination or reduction [32,33]. The formation of cobalt–aluminate was difficult and impractical to reduce at the temperatures used here and was therefore inactive towards the reductive amination. The reduced metal surface area of cobalt was largest for Co(23)/Al<sub>2</sub>O<sub>3</sub> at ca. 2.2 m<sup>2</sup> g<sub>catalyst</sub><sup>-1</sup> and was correlated with 2-propanol conversion (Table 2).

### 3.2. Reductive amination of 2-propanol

The conversions of 2-propanol and selectivities to MIPA, acetone, DIPA, and DIPE in the reductive amination of 2-propanol on Co/γ-Al<sub>2</sub>O<sub>3</sub> catalysts were tested at cobalt loadings of 4–27 wt% (Table 3). The 2-propanol conversions over these catalysts ranged from 32.4 to 81.5%. The conversion increased with the increase of cobalt loading, but after reaching 23 wt% Co the conversion decreased. Although the conversion is not directly proportional to the metallic surface area of Co/γ-Al<sub>2</sub>O<sub>3</sub> catalyst the observed variation in the conversion can be correlated to the difference in the reduced metallic surface area of the catalysts. This was likely due to variations of reducibility and cobalt metal dispersion accompanying the higher metallic surface areas [34], which was shown by the H<sub>2</sub>-chemisorption results (Table 2). The sum of the selectivities to MIPA and acetone as main products was almost constant at ca. 97% under the tested operating conditions. Small quantities of DIPA were formed by the consecutive reaction of MIPA with 2-propanol. Also, DIPE was formed by the condensation/dehydration of 2-propanol. The selectivity pattern was similar to those over other catalysts for reductive amination [35]. Various by-products which could be formed by the condensation, decarbonylation, disproportionation and hydrogenolysis of 2-propanol under the tested operating conditions were C<sub>1</sub>–C<sub>2</sub> compounds, DIPE and DIPA. However, the quantities formed here were negligible during the reductive amination of 2-propanol.

The effects of hydrogen partial pressure were examined at 210 °C with a space velocity of 4.29 h<sup>-1</sup> and R = [2-propanol]:[NH<sub>3</sub>] molar ratio of 1:4 in the reductive amination of 2-propanol over Co(23)/Al<sub>2</sub>O<sub>3</sub> catalyst (Fig. 3). The total flow rate was 90 cm<sup>3</sup> min<sup>-1</sup>. To maintain constant partial pressures of the other reactants, nitrogen was used as diluent. At H<sub>2</sub> partial pressures below 18 kPa,

**Table 3**  
Effect of cobalt content in the reductive amination of 2-propanol over Co/ $\gamma$ -Al<sub>2</sub>O<sub>3</sub>.<sup>a</sup>

Catalyst	Conversion <sup>b</sup> (%)	Selectivity (%)				MIPA yield (%)
		MIPA	Acetone	DIPA <sup>c</sup>	DIPE <sup>d</sup>	
Co(4)/Al <sub>2</sub> O <sub>3</sub>	32.4	76.1	21.8	–	2.1	24.7
Co(11)/Al <sub>2</sub> O <sub>3</sub>	76.4	72.5	25.0	0.2	2.3	55.4
Co(17)/Al <sub>2</sub> O <sub>3</sub>	78.1	71.2	25.9	0.4	2.3	55.6
Co(23)/Al <sub>2</sub> O <sub>3</sub>	81.5	71.7	25.9	0.2	2.3	58.4
Co(27)/Al <sub>2</sub> O <sub>3</sub>	80.3	71.7	25.6	0.2	2.5	57.6

<sup>a</sup> Reaction conditions:  $T = 210^\circ\text{C}$ ,  $\text{WHSV} = 4.29\text{ h}^{-1}$ ; feed compositions of 2-propanol/ $\text{NH}_3/\text{H}_2/\text{N}_2$  (mol ratio) = 1/4/6/22.8.

<sup>b</sup> Conversion and selectivities to MIPA, acetone, DIPA, and DIPE obtained at 5 min on stream.

<sup>c</sup> DIPA, diisopropylamine.

<sup>d</sup> DIPE, diisopropyl ether.

conversion increased rapidly with increasing H<sub>2</sub> partial pressure; above this, increasing H<sub>2</sub> partial pressure resulted in a slight increase of conversion. Decreasing H<sub>2</sub> partial pressure progressively deactivated the catalyst, possibly due to the formation of cobalt nitride by strongly adsorbed nitrogen species on the cobalt metal ( $3\text{Co} + \text{NH}_3 \rightarrow \text{Co}_3\text{N} + 1.5\text{H}_2$ ) [5,36]. Excess hydrogen efficiently hindered the phase transition of the catalyst to metal nitride during the reaction and prevented the deactivation of the catalyst. MIPA selectivity increased progressively with increasing H<sub>2</sub> partial pressure and selectivities to acetone and DIPE decreased. This is consistent with the postulated reaction mechanism whereby the imine intermediate must first be hydrogenated to form amine before further reactions can occur [5].

The effects of ammonia partial pressure on the reductive amination of 2-propanol over Co(23)/ $\gamma$ -Al<sub>2</sub>O<sub>3</sub> was investigated at 210 °C with a space velocity of 4.29 h<sup>-1</sup> and  $R = [\text{2-propanol}]:[\text{H}_2]$  molar ratio of 1:8 (Fig. 4). 2-Propanol conversion was almost constant with increasing ammonia partial pressure. MIPA selectivity increased progressively with increasing ammonia partial pressure and acetone selectivity decreased. Excess ammonia had a positive effect on MIPA selectivity by the reductive amination of acetone, limiting the production of DIPA, DIPE and acetone [37–39].

Reaction temperatures of 170–250 °C were adopted at 2-propanol WHSV of 4.29 h<sup>-1</sup> and 2-propanol: $\text{NH}_3:\text{H}_2$  molar ratio of 1:6:12 (Fig. 5). The total flow rate of 90 cm<sup>3</sup> min<sup>-1</sup> was maintained by controlling the nitrogen flow. The 2-propanol conversion increased with increasing reaction temperature. The MIPA selectivity decreased with the increase of the reaction temperature as opposed to the conversion and selectivity to acetone. At high temperature, the formation of acetone was favored by the dehydrogenation of 2-propanol. The maximum yield of MIPA was

ca. 79%, at 190 °C. Decreasing amine selectivity was observed at high temperature due to strong enhancement of side reactions, i.e. the dehydrogenation of corresponding alcohols and the disproportion of reactant and product amines [5,34,37–39]. As discussed above, acetone is the first product of 2-propanol dehydrogenation as shown in Scheme 1. High performance for the reductive amination of acetone to MIPA would be possible at lower reaction temperature than that of 2-propanol. The water vapor as another compound produced during the dehydroamination of acetone was

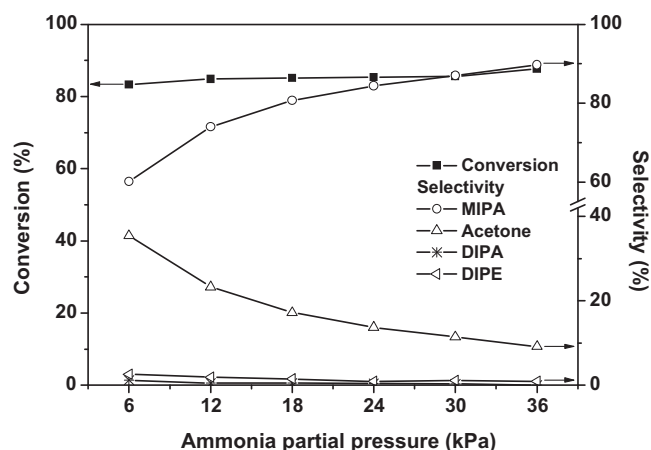


**Fig. 4.** Influence of ammonia partial pressure on the reductive amination of 2-propanol over Co(23)/Al<sub>2</sub>O<sub>3</sub>. Reaction conditions:  $T = 210^\circ\text{C}$ ,  $\text{WHSV} (\text{h}^{-1}) = 4.29$ ; feed composition of 2-propanol/ $\text{H}_2$  (mol%) = 1/8.

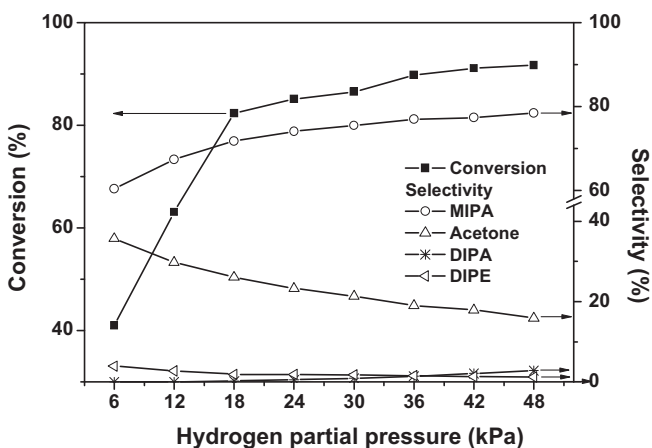


**Fig. 3.** Effects of hydrogen partial pressure on the reductive amination of 2-propanol over Co(23)/Al<sub>2</sub>O<sub>3</sub>. Reaction conditions:  $T = 210^\circ\text{C}$ ,  $\text{WHSV} (\text{h}^{-1}) = 4.29$ ; feed compositions of 2-propanol/ $\text{NH}_3$  (mol%) = 1/4.

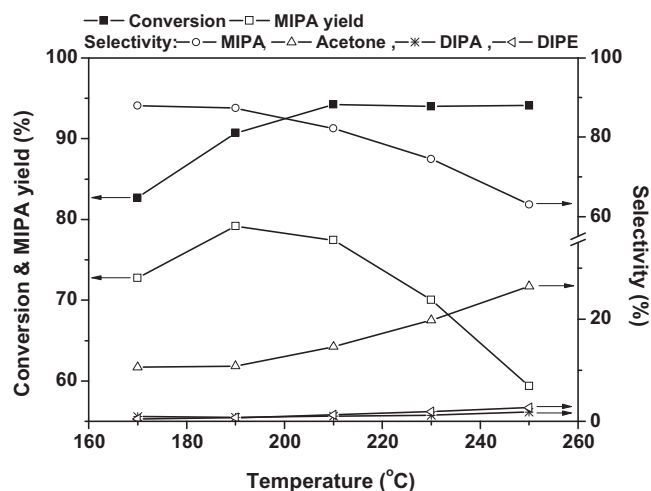


**Fig. 5.** Effects of reaction temperature on the reductive amination of 2-propanol over Co(23)/Al<sub>2</sub>O<sub>3</sub>. Reaction conditions:  $\text{WHSV} (\text{h}^{-1}) = 4.29$ ; feed composition of 2-propanol/ $\text{NH}_3/\text{H}_2/\text{N}_2$  (mol%) = 1/6/12/14.8.

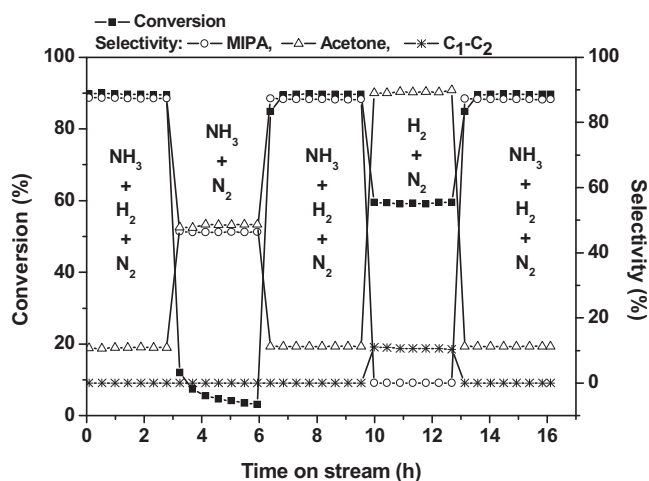


**Fig. 6.** Evolution of 2-propanol conversion and MIPA selectivity as a function of time on stream in the presence or absence of hydrogen for the reductive amination of 2-propanol over Co(23)/Al<sub>2</sub>O<sub>3</sub>. During the reaction, the flow of the N<sub>2</sub> + H<sub>2</sub> mixture was changed to pure N<sub>2</sub> and then returned to its initial composition. Reaction conditions: *T* = 190 °C, WHSV = 4.29 h<sup>-1</sup>; feed composition of 2-propanol/NH<sub>3</sub>/H<sub>2</sub>/N<sub>2</sub> (mol%) = 1/6/12/14.8, 1/6/0/26.8.

not examined in this study. However, only slight influence of water vapor in yield of amine product has been reported on the catalytic amination of 1-methoxy-2-propanol over silica supported catalyst [37].

To observe the effect of deactivation, the evolution of 2-propanol conversion and selectivities to MIPA, acetone and C<sub>1</sub>–C<sub>2</sub> products were investigated over Co(23)/Al<sub>2</sub>O<sub>3</sub> catalyst with respect to time on stream in the presence or absence of NH<sub>3</sub> or H<sub>2</sub> (Fig. 6). During the reaction, the flow of NH<sub>3</sub> or H<sub>2</sub> was stopped and returned to the initial flow composition. When amination was performed with initial feed compositions of 2-propanol/NH<sub>3</sub>/H<sub>2</sub>/N<sub>2</sub> (mol ratio) = 1/6/12/14.8, 2-propanol conversion and selectivities to MIPA and acetone were 90%, 88%, and 11%, respectively. Removing the H<sub>2</sub> flow from the reactant stream rapidly deactivated the catalyst and no formation of MIPA was observed within 1 h on stream. However, the initial activity and selectivities to MIPA and acetone were completely recovered upon re-exposure to feed containing hydrogen. Also, no deactivation of the catalyst was shown. Verhaak et al. [40] observed the rapid deactivation of supported nickel catalyst in the disproportionation of *n*-propylamine when hydrogen in the feed was replaced by nitrogen. In this study similar result was observed. The conversion and selectivity were totally regenerated when the gas feed containing hydrogen was replaced once again. They ascribed this deactivation to the formation of metal nitride during the reaction in nitrogen. The formation of metal nitride can deactivate metallic catalysts used for reductive amination [41]. Feed containing excess hydrogen could efficiently hinder the phase transition of the metallic catalyst to nitride during the reaction, preventing deactivation. A reactant flow without NH<sub>3</sub> resulted in the synthesis of acetone as the main product of the dehydrogenation of 2-propanol in the presence of H<sub>2</sub>; propylene was detected as a minor product and negligible amounts of methane and ethylene were also observed from the hydrogenolysis of C<sub>3</sub> compounds. The only alumina support gave products of propylene and DIPE, which formed on weakly acidic sites [42,43]. After adding NH<sub>3</sub> to the reactants, the initial conversion of 2-propanol and selectivities to MIPA and acetone over Co/Al<sub>2</sub>O<sub>3</sub> catalyst were completely recovered.

To assess the adsorbed species during the amination reaction and the origin of deactivation, NH<sub>3</sub>-TPD and simultaneous NH<sub>3</sub>-TPD and H<sub>2</sub>-TPR experiments were conducted using a quadruple mass spectrometer. Argon and a mixture of hydrogen and argon

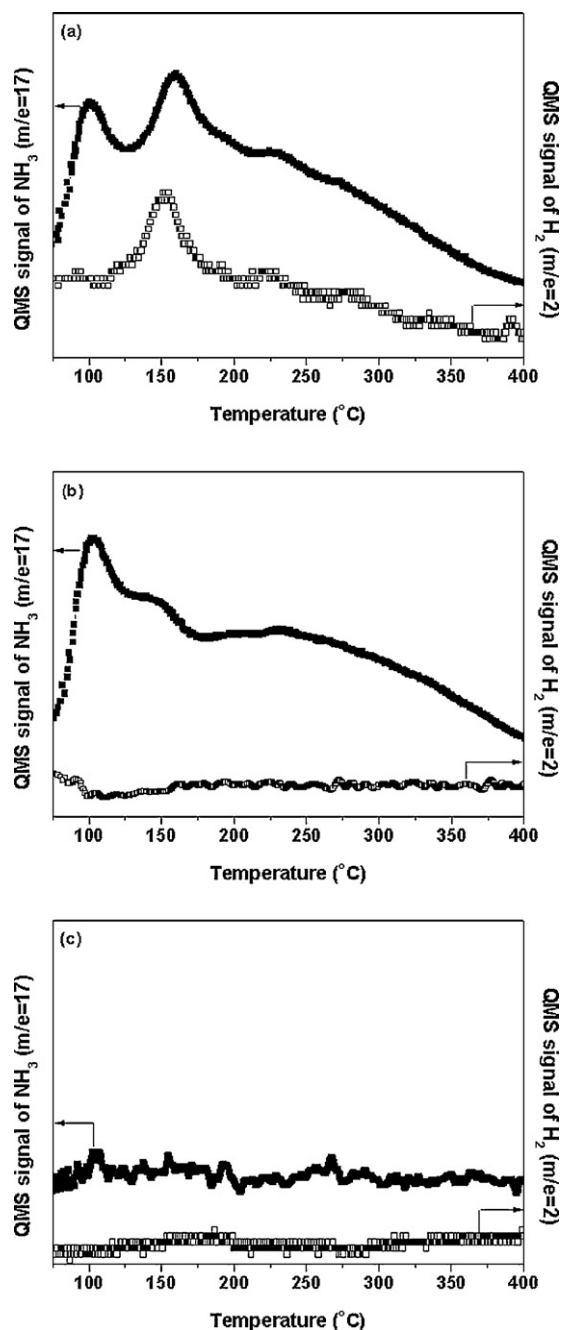


**Fig. 7.** Evolution of NH<sub>3</sub> and H<sub>2</sub> during TPD/TPR for Co(23)/Al<sub>2</sub>O<sub>3</sub> catalyst under flowing (a) 5% H<sub>2</sub>/Ar, (b) Ar, and (c) 5% H<sub>2</sub>/Ar. The samples reduced were pretreated under flowing ((a) and (b)) 20% NH<sub>3</sub>/N<sub>2</sub> or (c) 4% NH<sub>3</sub>/16% H<sub>2</sub>/N<sub>2</sub> at 190 °C for 12 h.

were used. Prior to each experiment, samples were reduced under a H<sub>2</sub> flow at 600 °C for 3 h with heating at 10 °C min<sup>-1</sup>. Fig. 7 shows the evolution of NH<sub>3</sub> and H<sub>2</sub> during TPD/TPR using Co(23)/Al<sub>2</sub>O<sub>3</sub> catalyst under H<sub>2</sub>/Ar and Ar flows. The reduced samples were pretreated under flowing 20% NH<sub>3</sub>/N<sub>2</sub> or 4% NH<sub>3</sub>/16% H<sub>2</sub>/N<sub>2</sub> at 190 °C for 12 h. Pure Ar was then passed through the reactor for 15 min. NH<sub>3</sub> desorption and H<sub>2</sub> consumption were recorded under flowing 5% H<sub>2</sub>/Ar for the sample pretreated with 20% NH<sub>3</sub>/N<sub>2</sub> (Fig. 7(a)). The NH<sub>3</sub>-TPD profiles of the sample pretreated with NH<sub>3</sub>/Ar show two main peaks at 110 and 170 °C and broad peaks up to 400 °C. The first peak originated from the desorption of weakly adsorbed ammonia on the surface of the metal phase and alumina support; the second one corresponds to the desorption of strongly adsorbed ammonia

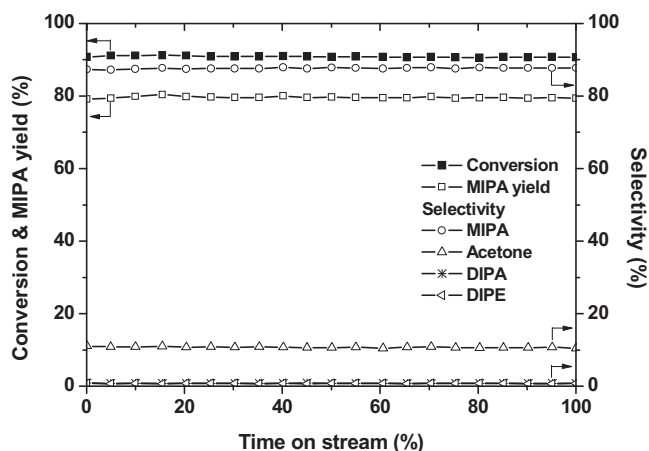


**Fig. 8.** Long-term stability of Co(23)/Al<sub>2</sub>O<sub>3</sub> for reductive amination. Reaction conditions:  $T = 190\text{ }^{\circ}\text{C}$ ,  $\text{WHSV} = 4.29\text{ h}^{-1}$ ; feed composition of 2-propanol/NH<sub>3</sub>/H<sub>2</sub>/N<sub>2</sub> (mol%) = 1/6/12/14.8.

on the cobalt, which may be due to the formation of surface cobalt nitride [44]. The hydrogen consumption peak at  $160\text{ }^{\circ}\text{C}$  indicates the removal of strongly adsorbed nitrogen-containing surface species in the presence of hydrogen. To investigate the role of hydrogen in the amination reaction, NH<sub>3</sub>-TPD was performed under flowing Ar in the absence of hydrogen (Fig. 7(b)). When only Ar was used during TPD, the second peak was smaller, indicating the facile removal of strongly adsorbed nitrogen-containing surface species in the presence of hydrogen. H<sub>2</sub> evolution was not detected during NH<sub>3</sub>-TPD. The evolution of NH<sub>3</sub> or H<sub>2</sub> was not observed over the sample pretreated with 4% NH<sub>3</sub>/16% H<sub>2</sub>/N<sub>2</sub>, indicating that hydrogen was linked to the prevention of catalyst deactivation due to surface nitride formation [5,40,41,44,45].

The long term stability of the Co(23)/Al<sub>2</sub>O<sub>3</sub> catalyst during the reductive amination of 2-propanol was assessed (Fig. 8). The Co(23)/ $\gamma$ -Al<sub>2</sub>O<sub>3</sub> catalyst which showed the best catalytic activity among the catalysts studied here exhibited constant conversion and selectivities to MIPA and acetone up to 100 h on stream. The Co/ $\gamma$ -Al<sub>2</sub>O<sub>3</sub> catalyst showed good catalytic activity and stability, making its use economically viable.

#### 4. Conclusions

The Co/ $\gamma$ -Al<sub>2</sub>O<sub>3</sub> catalysts with 4–27 wt% cobalt loadings were prepared by incipient-wetness impregnation. Particle sizes increased from 12.5 to 21.5 nm with increasing cobalt content. Larger cobalt oxide particles could be more easily reduced due to weaker interactions with the support. The highly reduced cobalt metal surface area could be correlated with the enhancement of 2-propanol conversion. Excess ammonia enhanced 2-propanol conversion and MIPA selectivity. Excess hydrogen hindered the phase transition of the catalyst to metal nitride during reaction and the deactivation of the catalyst. The Co/ $\gamma$ -Al<sub>2</sub>O<sub>3</sub> catalyst showed good catalytic performance and its catalytic activities were stable in the presence of excess hydrogen and ammonia under atmospheric pressure.

#### Acknowledgement

This work was financially supported by a grant from the Industrial Source Technology Development Programs (2008-10031908) of the Ministry of Knowledge Economy (MKE) of Korea.

#### References

- [1] K.S. Hayes, Appl. Catal. A: Gen. 221 (2001) 187–195.
- [2] R. Vultier, A. Baiker, A. Wokaun, Appl. Catal. 30 (1987) 167–176.
- [3] A. Fischer, T. Mallat, A. Baiker, Angew. Chem. Int. Ed. 38 (1999) 351–354.
- [4] M. Pérez-Mendoza, M. Domingo-García, F.J. López-Garzón, Appl. Catal. A: Gen. 224 (2002) 239–253.
- [5] G. Sewell, C. O'Connor, E. Steen, Appl. Catal. A: Gen. 125 (1995) 99–112.
- [6] J. Becker, J.P.M. Niederer, M. Keller, W.F. Hölderich, Appl. Catal. A: Gen. 197 (2000) 229–238.
- [7] G. Boettger, H. Corr, H. Hoffmann, H. Toussaint, S. Winderl, US Patent, 4,014,933 (1977).
- [8] H.Y. Jeon, C.-H. Shin, H.J. Jung, S.B. Hong, Appl. Catal. A: Gen. 305 (2006) 70–78.
- [9] K.V.R. Chary, K.K. Seel, D. Naresh, P. Ramakanth, Catal. Commun. 9 (2008) 75–81.
- [10] G. Sewell, C. O'Connor, E. Steen, J. Catal. 167 (1997) 513–521.
- [11] G.A. Vedage, L.A. Emig, H.X. Li, J.N. Armor, US Patent 5,917,092 (1999).
- [12] G.A. Vedage, K.S. Hayes, M. Leeaphon, J.N. Armor, US Patent 5,932,769 (1999).
- [13] A. Fischer, T. Mallat, A. Baiker, Catal. Today 37 (1997) 167–189.
- [14] C. Dume, W.F. Hölderich, Appl. Catal. A: Gen. 183 (1999) 167–176.
- [15] M.E. Domínea, M.C.H. Sotoa, Y. Perez, Catal. Today 159 (2011) 2–11.
- [16] H. Kimura, K. Ishikawa, K. Nishino, S. Nomura, Appl. Catal. A: Gen. 286 (2005) 120–127.
- [17] C.U. Kim, Y.S. Kim, H.J. Chae, K.E. Jeong, S.Y. Jeong, K.W. Jun, K.Y. Lee, Korean J. Chem. Eng. 27 (2010) 777–784.
- [18] S. Zafeirotos, T. Dintzer, D. Teschner, R. Blume, M. Havecker, A. Knop-Gericke, R. Schlögl, J. Catal. 269 (2010) 309–317.
- [19] D.S. Kim, Y.H. Kim, J.E. Yie, E.D. Park, Korean J. Chem. Eng. 27 (2010) 822–827.
- [20] S.H. Kang, K.J. Woo, J.W. Bae, K.W. Jun, Y. Kang, Korean J. Chem. Eng. 26 (2009) 1533–1538.
- [21] P. Khemthong, W. Klysubun, S. Prayoonpokarach, F. Roessner, J. Wittayakun, J. Ind. Eng. Chem. 16 (2010) 531–538.
- [22] D.A. Gardner, R.T. Clark, US Patent 4,255,357 (1981).
- [23] I.D. Dobson, W.A. Lidy, P.S. Williams, US Patent 4,912,260 (1990).
- [24] B. Tijsebaert, B. Yilmaz, U. Müller, H. Gies, W. Zhang, X. Bao, F.S. Xiao, T. Tatsumi, D.D. Vos, J. Catal. 278 (2011) 246–252.
- [25] D.R. Corbin, S. Schwarz, G.C. Sonnichsen, Catal. Today 37 (1997) 71–102.
- [26] J.T. Richardson, W.C. Lu, J. Catal. 42 (1976) 275–281.
- [27] J.W. Bae, S.M. Kim, S.H. Kang, K.V.R. Chary, Y.J. Lee, H.J. Kim, K.W. Jun, J. Mol. Catal. A 311 (2009) 7–16.
- [28] M.M. Yung, E.M. Holmgreen, U. Ozkan, J. Catal. 247 (2007) 356–367.
- [29] G. Jacobs, Y. Ji, B.H. Davis, D. Cronauer, A.J. Kropf, C.L. Marshall, Appl. Catal. A: Gen. 333 (2007) 177–191.
- [30] A. Tavasoli, R.M.M. Abbaslou, M. Trepanier, A.K. Dalai, Appl. Catal. A: Gen. 345 (2008) 134–142.
- [31] Y. Ji, Z. Zhao, A. Duan, G. Jiang, J. Liu, J. Phys. Chem. C 113 (2009) 7186–7199.
- [32] L. Zhang, L. Dong, W. Yu, L. Liu, Y. Deng, B. Liu, H. Wana, F. Gao, K. Sun, L. Dong, J. Colloid Interface Sci. 355 (2011) 464–471.
- [33] J.W. Bae, S.M. Kim, Y. Jo Lee, M.J. Lee, K.W. Jun, Catal. Commun. 10 (2009) 1358–1362.
- [34] A.K. Rausch, E. Steen, F. Roessner, J. Catal. 253 (2008) 111–118.
- [35] V. Zamylny, L. Kubelkova, E. Baburek, K. Jiratova, J. Novakova, Appl. Catal. A: Gen. 169 (1998) 119–125.
- [36] A. Baiker, I. Monti, Y. Songfan, J. Catal. 88 (1984) 81–88.
- [37] V.A. Bassili, A. Baiker, Appl. Catal. 65 (1990) 293–308.
- [38] S.R. Kirumakki, M. Papadaki, K.V.R. Chary, N. Nagarajua, J. Mol. Catal. A 321 (2010) 15–21.
- [39] A. Fischer, M. Maciejewski, T. Bürgi, T. Mallat, A. Baiker, J. Catal. 183 (1999) 373–383.
- [40] M.J.F.M. Verhaak, A.J. van Dillen, J.W. Geus, Appl. Catal. A: Gen. 109 (1994) 263–275.
- [41] M.J.F.M. Verhaak, A.J. van Dillen, J.W. Geus, J. Catal. 143 (1993) 187–200.
- [42] C.R. Narayanan, S. Srinivasan, A.K. Datye, R. Gorte, A. Biaglow, J. Catal. 138 (1992) 659–674.
- [43] S. Srinivasan, C.R. Narayanan, A. Biaglow, R. Gorte, A.K. Datye, Appl. Catal. A: Gen. 132 (1995) 271–287.
- [44] A. Baiker, J. Kijenski, Catal. Rev. Sci. Eng. 27 (1985) 653–697.
- [45] J. Kritzenberger, E. Jobson, A. Wokaun, A. Baiker, Catal. Lett. 5 (1990) 73–80.